




Zika virus alters centrosome organization to suppress the innate immune response

Andrew Kodani^{1,*†} , Kristeene A Knopp^{2,3,†} , Elizabeth Di Lullo^{4,5}, Hanna Retallack^{2,3}, Arnold R Kriegstein^{4,5}, Joseph L DeRisi^{2,3} & Jeremy F Reiter^{2,3,6} 

Abstract

Zika virus (ZIKV) is a flavivirus transmitted via mosquitoes and sex to cause congenital neurodevelopmental defects, including microcephaly. Inherited forms of microcephaly (MCPH) are associated with disrupted centrosome organization. Similarly, we found that ZIKV infection disrupted centrosome organization. ZIKV infection disrupted the organization of centrosomal proteins including CEP63, a MCPH-associated protein. The ZIKV nonstructural protein NS3 bound CEP63, and expression of NS3 was sufficient to alter centrosome architecture and CEP63 localization. Loss of CEP63 suppressed ZIKV-induced centrosome disorganization, indicating that ZIKV requires CEP63 to disrupt centrosome organization. ZIKV infection or CEP63 loss decreased the centrosomal localization and stability of TANK-binding kinase 1 (TBK1), a regulator of the innate immune response. ZIKV infection also increased the centrosomal accumulation of the CEP63 interactor DTX4, a ubiquitin ligase that degrades TBK1. Therefore, we propose that ZIKV disrupts CEP63 function to increase centrosomal DTX4 localization and destabilization of TBK1, thereby tempering the innate immune response.

Keywords centrosome; innate immunity; microcephaly; Zika virus

Subject Categories Cell Adhesion, Polarity & Cytoskeleton; Immunology; Microbiology, Virology & Host Pathogen Interaction

DOI 10.15252/embr.202052211 | Received 3 December 2020 | Revised 31 May 2022 | Accepted 15 June 2022 | Published online 6 July 2022

EMBO Reports (2022) 23: e52211

Introduction

In the summer of 2015, cerebral malformations were linked to mosquito-transmitted Zika virus (ZIKV). Inherited forms of microcephaly (MCPH) are characterized by reduced head and brain size, resulting in severe intellectual disability and motor movement defects. Many forms of MCPH are caused by autosomally

recessive mutations in genes encoding centrosomal proteins required for centrosome biogenesis and mitotic progression (Jayaraman *et al*, 2018). Given the similar pathologies between ZIKV-associated and inherited MCPH, we hypothesized that both disorders were due to centrosomal defects leading to disrupted brain development.

In mammalian cells, centrosomes serve as the microtubule organizing center of the cell to facilitate neuronal migration and cell division (Nano & Basto, 2017; Bertipaglia *et al*, 2018; Saade *et al*, 2018). The centrosome is composed of centrioles surrounded by a pericentrosomal matrix that nucleates microtubules (Varadaraman & Rusan, 2018; Gonczy & Hatzopoulos, 2019). During S phase, the centrosome duplicates by recruiting specialized proteins to the centriole base (Sir *et al*, 2011; Brown *et al*, 2013; Gonczy & Hatzopoulos, 2019; Kim *et al*, 2019). Many MCPH-associated proteins are recruited to the centrosome in a hierarchical manner to promote centrosome duplication (Sir *et al*, 2011; Lawo *et al*, 2012; Sonnen *et al*, 2013; Kodani *et al*, 2015; Jayaraman *et al*, 2016). Defects in centrosome organization and biogenesis leading to cell death or premature differentiation in neural progenitors may underlie the pathology of many forms of MCPH (Bazzi & Anderson, 2014; Hu *et al*, 2014; Jayaraman *et al*, 2016).

Cells infected with ZIKV have disrupted centrosome organization and mitotic abnormalities, leading to altered neural progenitor differentiation (Souza *et al*, 2016; Gabriel *et al*, 2017; Wolf *et al*, 2017; Ferraris *et al*, 2019; Kesari *et al*, 2020). However, the mechanism by which ZIKV disrupts centrosome architecture remains unclear. We found that ZIKV alters the function of the MCPH-associated protein, CEP63. More specifically, the ZIKV nonstructural protein, NS3, localizes to the centrosome and binds CEP63. ZIKV NS3 overaccumulates CEP63 at centrosomes of ZIKV-infected cells and recruits the ubiquitin ligase DTX4. DTX4 promotes the degradation of TBK1, a regulator of the innate immune response (Fitzgerald *et al*, 2003; Perry *et al*, 2004; Li *et al*, 2011; Wang *et al*, 2012; Liu *et al*, 2015). Consequently, ZIKV-infected cells express lower levels of interferon β (IFN β), a key antiviral signal. We propose that ZIKV recruits

¹ Department of Cell and Molecular Biology, Center for Pediatric Neurological Disease Research, St. Jude Children's Research Hospital, Memphis, TN, USA

² Department of Biochemistry and Biophysics, University of California, San Francisco, San Francisco, CA, USA

³ Chan Zuckerberg Biohub, San Francisco, CA, USA

⁴ Eli and Edythe Broad Center of Regeneration Medicine and Stem Cell Research, University of California, San Francisco, San Francisco, CA, USA

⁵ Department of Neurology, University of California, San Francisco, San Francisco, CA, USA

⁶ Cardiovascular Research Institute, University of California, San Francisco, San Francisco, CA, USA

*Corresponding author. Tel: +1 901 595 2522; E-mail: andrew.kodani@stjude.org

†These authors contributed equally to this work

CEP63 to the centrosome to degrade TBK1, dampening antiviral responses.

Results and Discussion

ZIKV infection disorganizes the centrosome

To explore whether microcephaly associated with ZIKV infection involves the centrosome, we infected human-induced neural precursor cells (iNPCs) derived from induced pluripotent stem cells with ZIKV and examined the organization of their centrosomes. Sixteen hours post infection (hpi) with ZIKV, iNPCs displayed supernumerary foci of Centrin, a component of the centriolar distal lumen (Paoletti *et al*, 1996; Fig 1A and C). The supernumerary foci began to

appear 10 hpi and peaked at 16 hpi. Similarly, ZIKV-infected U87 and H4 cells exhibited supernumerary Centrin foci (Figs 1B and C, and EV1A). Like ZIKV-infected cultured cells, NPCs isolated from human fetal neocortical tissue infected by ZIKV exhibited supernumerary Centrin foci (Fig 1D). Twenty-four hours post infection, the Centrin foci relocated to the cytoplasm in the vicinity of the endoplasmic reticulum where ZIKV replication occurs (Xing *et al*, 2020; Zhang *et al*, 2016; Fig EV1B and C).

In ZIKV-infected iNPCs and U87 cells, the supernumerary Centrin foci co-localized with the distal centriole protein CP110 (Spektor *et al*, 2007) and centriolar satellite protein, CEP90 which is associated with microcephaly and Joubert syndrome (Figs 1E and EV1D), indicating that ZIKV-associated supernumerary Centrin foci can recruit centrosome-associated proteins. However, the supernumerary Centrin foci do not accumulate the distal appendage protein

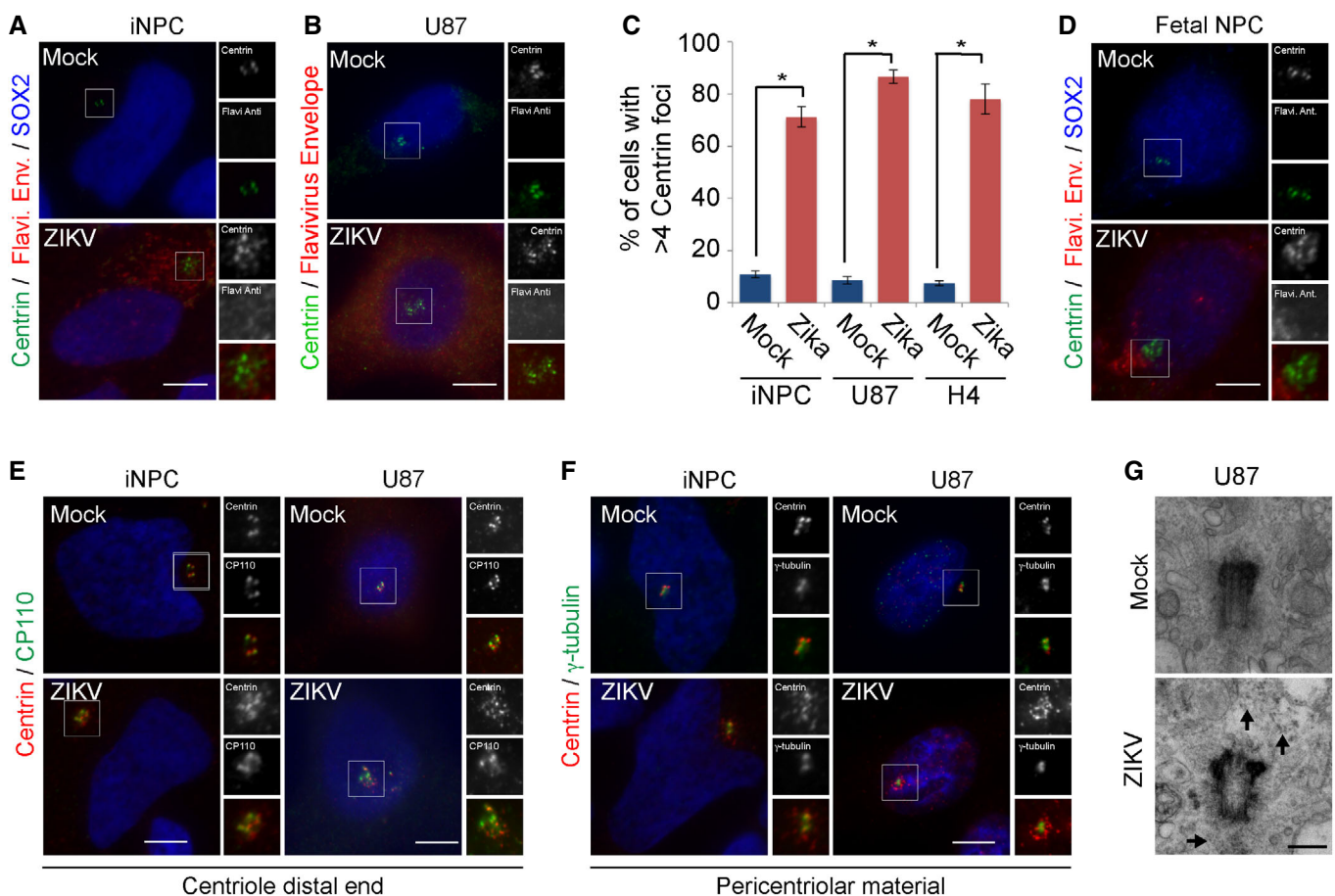


Figure 1. ZIKV infection induces the formation of supernumerary Centrin foci in neural precursor cells.

- A Neural precursors derived from human iPS cells (iNPCs) were mock or ZIKV-infected and co-stained for Centrin (green), Sox2 (blue), and flavivirus envelope (red). All cells were fixed 16 h post infection (hpi).
- B Mock and ZIKV-infected U87 and H4 cells in S phase co-stained for Centrin (green), flavivirus envelope (red) and DNA (blue).
- C Quantification of the percentage of mock or ZIKV-infected iNPC, U87 or H4 cells in S phase with greater than four Centrin foci. Bars represent the mean \pm SD normalized to the control. Asterisk denotes $P < 0.005$ (Student's *t*-test). Three biological replicates are represented.
- D Neural precursor cells mock or ZIKV-infected and co-stained for Centrin (green), flavivirus envelope (red), and Sox2 (blue).
- E Mock or ZIKV-infected iNPC and U87 cells in S phase co-stained for Centrin (red) and the centriole distal end component, CP110 (green).
- F Mock or ZIKV-infected iNPC and U87 cells co-stained for Centrin (red) and the pericentriolar material proteins γ -tubulin (green).
- G Transmission electron micrographs of centrioles from mock or ZIKV-infected U87 cells.

Data information: Scale bars indicate 100 nm. Arrows indicate electron-dense particles.

CEP164 (Graser *et al*, 2007) or pericentrosomal protein γ -tubulin (Stearns *et al*, 1991; Figs 1F, and EV1E and F). ZIKV infection did not alter the levels of CP110 or γ -tubulin (Fig EV1G). Electron microscopy revealed that ZIKV infection did not alter centriole number or distal appendages 16 hpi (Fig 1G). Instead, ZIKV-infected cells accumulated electron-dense particles in the vicinity of the centrosome. Thus, acute ZIKV infection does not cause centrosome overproduction, but rather disorganizes the centrosome.

ZIKV disrupts centrosome organization in a CEP63-dependent manner

Many MCPH-associated proteins dynamically localize to the centrosome during its biogenesis (Kumar *et al*, 2009; Khan *et al*, 2014; Martin *et al*, 2014). Given that ZIKV infection alters centrosome organization, we investigated whether the localization of MCPH-associated proteins is also altered. ZIKV infection in U87 cells did not affect either the localization or the levels of the MCPH-associated proteins PLK4, STIL, SAS6, CDK5RAP2, CEP152, or WDR62 (Fig EV2A–D). In striking contrast, ZIKV infection caused CEP63, another MCPH-associated protein (Sir *et al*, 2011), to overaccumulate in the proximity of supernumerary Centrin foci (Fig 2A, and quantified in Fig 2B). As in U87 cells, ZIKV infection of iNPCs and NPCs isolated from dissociated fetal brain tissue relocalized CEP63 near supernumerary Centrin foci (Fig 2C). Although ZIKV infection did not dramatically affect CEP63 protein levels, it did increase the levels of a higher molecular weight species of CEP63 (Fig 2D). There was a decrease in CEP63 localized at the centrosome in ZIKV-infected cells (Quantified in Fig EV2E and F) suggesting that ZIKV distributes CEP63 away from the centrosome.

Because MCPH-associated proteins function in centrosome biogenesis, we hypothesized that the disruption of CEP63 localization participates in ZIKV-associated centrosomal disorganization. To test this, we infected control and *Cep63^{gt/gt}* mouse embryonic fibroblasts (MEFs; Brown *et al*, 2013) with ZIKV and assessed Centrin organization. The *Cep63^{gt/gt}* cells were developed and first characterized by Brown *et al* and we confirmed the absence of *Cep63* in *Cep63^{gt/gt}* (Brown *et al*, 2013) cells using immunofluorescence and WB (Fig EV2G and H). In contrast to control cells, ZIKV did not induce supernumerary Centrin foci in the absence of *Cep63* (Fig 2E and F). Together, these findings indicate that CEP63 is required for ZIKV-associated reorganization of the centrosome.

ZIKV NS3 binds CEP63 to disrupt centrosome organization

Overexpression studies have demonstrated that ZIKV NS3 localizes in the proximity of the centrosome and associates with centrosomal proteins (Khadka *et al*, 2011; Hou *et al*, 2017; Coyaud *et al*, 2018). As centrosome organization is disrupted in ZIKV-infected cells, we investigated whether NS3 localizes to the centrosome in ZIKV-infected cells. In ZIKV-infected iNPCs, NS3 localized to one or two foci among the supernumerary Centrin foci between 10 and 16 hpi (Figs 3A and EV3A). ZIKV NS3 partially co-localized with CEP152 which localizes to the proximal centriole (Fig EV3B). In agreement with previous reports, NS3 was detected at the endoplasmic reticulum 24 hpi in ZIKV-infected cells (Xing *et al*, 2020; Fig EV1B and C). A yeast two-hybrid analysis suggested that CEP63 binds the non-structural protein NS3 of flaviviruses related to ZIKV (Le Breton

et al, 2011). As ZIKV infection causes CEP63 to overaccumulate near centrosomes to disrupt centrosome organization, we determined whether ZIKV NS3 interacts with CEP63. Immunoprecipitation of endogenous CEP63 in ZIKV-infected cells revealed that CEP63 interacts with ZIKV NS3 (Fig 3B). To confirm the interaction of ZIKV NS3 with CEP63, we transfected cells with Myc-tagged Brazilian ZIKV NS3 and found that Myc-NS3 co-precipitated with endogenous CEP63, but not CP110, another centrosomal protein that misaccumulates at the centrosome upon ZIKV infection (Fig 3C).

Because ZIKV NS3 interacts with CEP63, we investigated whether CEP63 was required to localize NS3 to the centrosome. To test this, we infected control and *Cep63^{gt/gt}* MEFs with ZIKV and examined NS3 localization 16 hpi. Similar to control cells, ZIKV NS3 localized to centrosomes in *Cep63^{gt/gt}* MEFs (Fig 3D) suggesting that NS3 affects CEP63 localization, but not vice versa.

NS3 acts together with another nonstructural protein, NS2B, to form a proteolytic complex (Fig 3E; Bera *et al*, 2007). To gain insight into how ZIKV disrupts centrosomes, we examined whether the NS2B/NS3 complex could induce supernumerary Centrin foci or if NS3 alone is sufficient. The expression of either Brazilian ZIKV Myc-NS2B/NS3 or Myc-NS3 induced supernumerary Centrin foci (Figs 3F–H and EV3C), suggesting NS3 alone is sufficient to perturb centrosome organization. Additionally, Myc-NS3 increased the centrosomal accumulation of CEP63 (Fig 3I and quantified in Fig EV3F) and had no effect on the localization or stability of CEP152, CDK5RAP2 and WDR62 (Figs 3I and EV3D and E). Therefore, Brazilian ZIKV NS3 interacts with CEP63, localizes to the centrosome, and is sufficient to reorganize centrosomal architecture akin to ZIKV infection.

Microcephaly is associated with South American strains of ZIKV, but not Uganda ZIKV (Calvet *et al*, 2016; Mlakar *et al*, 2016; Zhu *et al*, 2016). Given the NS3 proteins of the Brazilian and Ugandan strains of ZIKV differ by 11 amino acids, we examined whether Ugandan NS3 was sufficient to induce supernumerary Centrin foci and misrecruit CEP63. Like Brazilian NS3, Ugandan ZIKV NS3 localized to centrosomes (Fig 3J). In striking contrast to Brazilian ZIKV NS3, the Ugandan NS3 did not induce supernumerary Centrin foci or increase centrosomal CEP63 localization, instead lead to the loss of centrosomal composition (Fig 3J and quantified in Fig EV3G and H). Ugandan NS3 was unable to bind CEP63 and was expressed at the same levels as Brazilian NS3 (Fig EV3I and J) indicating that Brazilian ZIKV NS3 has acquired the ability to bind to and increase centrosomal CEP63 localization and induce supernumerary Centrin foci.

ZIKV suppresses innate immune signaling

To determine why ZIKV disrupts CEP63 function, we examined whether CEP63 interacts with proteins involved in host-pathogen pathways. Proximity interaction studies have suggested that CEP63 interacts with TBK1, a regulator of innate immunity (Gupta *et al*, 2015). Through co-immunoprecipitation, we confirmed that endogenous CEP63 and TBK1 interact (Fig 4A). During viral infections, the kinase TBK1 phosphorylates and activates the transcription factor IRF3, and is then degraded, to regulate interferon induction (Sharma *et al*, 2003; Cui *et al*, 2012; Liu *et al*, 2015). TBK1 localizes to centrosomes to promote centrosome organization and mitotic spindle formation (Farlik *et al*, 2012; Helgason *et al*, 2013; Gupta *et al*, 2015; Pillai *et al*, 2015; Onorati *et al*, 2016).

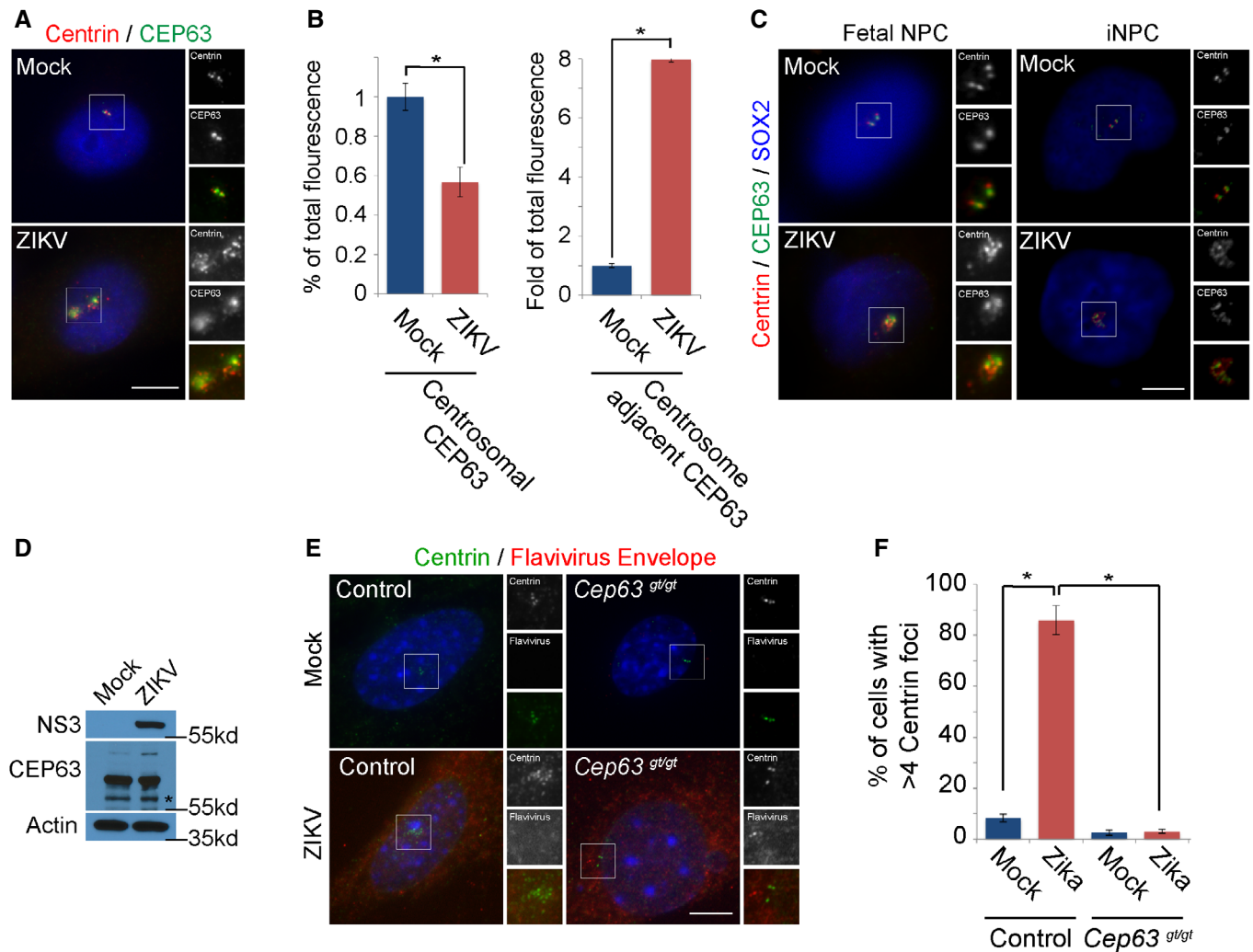


Figure 2. ZIKV induces supernumerary Centrin foci in a CEP63-dependent manner.

- A Mock or ZIKV-infected U87 cells in S phase co-stained for Centrin (red) and the centrosomal microcephaly-associated protein, CEP63 (green).
- B The fluorescence intensity \pm SD of CEP63 at the centrosome (0.5 μ m around the Centrin signal) and around the centrosome (1 μ m surrounding the Centrin signal minus the centrosomal CEP63) were quantified in mock and ZIKV-infected U87 cells. For fluorescence quantifications, eight cells were analyzed per experiment ($n = 3$). Asterisk denotes $P < 0.005$ (Student's t -test).
- C Mock and ZIKV-infected neuronal progenitors (NPC) isolated from fetal brain cortex and iPSC-derived neural precursor cells (iNPC) co-stained for Centrin (red), CEP63 (green), and SOX2 (blue).
- D Immunoblot analysis of lysate from mock or ZIKV-infected U87 cells probed for CEP63 and ZIKV NS3. Actin served as a loading control. Asterisk denotes specific band for CEP63.
- E S-phase mock and ZIKV-infected control and *Cep63^{gt/gt}* MEFs co-stained for Centrin (green) and flavivirus envelope (red).
- F Quantification of the percentage of mock or ZIKV-infected Het and *Cep63^{gt/gt}* MEFs in S phase with greater than four Centrin foci. Bars represent the mean \pm SD normalized to the control. Asterisk denotes $P < 0.005$ (Student's t -test). Three biological replicates are represented.

Data information: Scale bars indicate 5 μ m for all images. All cells were fixed 16 h post infection (hpi).

An activated form of TBK1, phospho-TBK1 (p-TBK1, Ser172), is removed from centrosomes upon ZIKV infection during mitosis (Onorati *et al*, 2016). We found that TBK1 and p-TBK1 localize to the centrosome during interphase and are absent from cells infected with ZIKV (Figs 4B and EV4A–C). ZIKV infection decreased levels of TBK1 and phosphorylated TBK1 (p-TBK1) at 16 hpi (Fig 4C).

As p-TBK1 is absent from centrosomes of ZIKV-infected cells, we assessed whether ZIKV infection impairs the induction of interferon beta (IFN β) using reverse-transcription digital droplet

PCR (RT-ddPCR). Following ZIKV infection, IFN β expression gradually peaked 6–8 hpi, (Fig 4D). IFN β expression was abruptly curtailed at 10 hpi in ZIKV-infected cells, corresponding to the timing of when ZIKV NS3 localizes to the centrosome (Fig EV3A). Therefore, we propose that ZIKV may suppress the innate immune response by suppressing TBK1 stability and centrosome organization.

To test whether ZIKV disrupts TBK1 function in a CEP63-dependent manner, we examined whether centrosomal p-TBK1

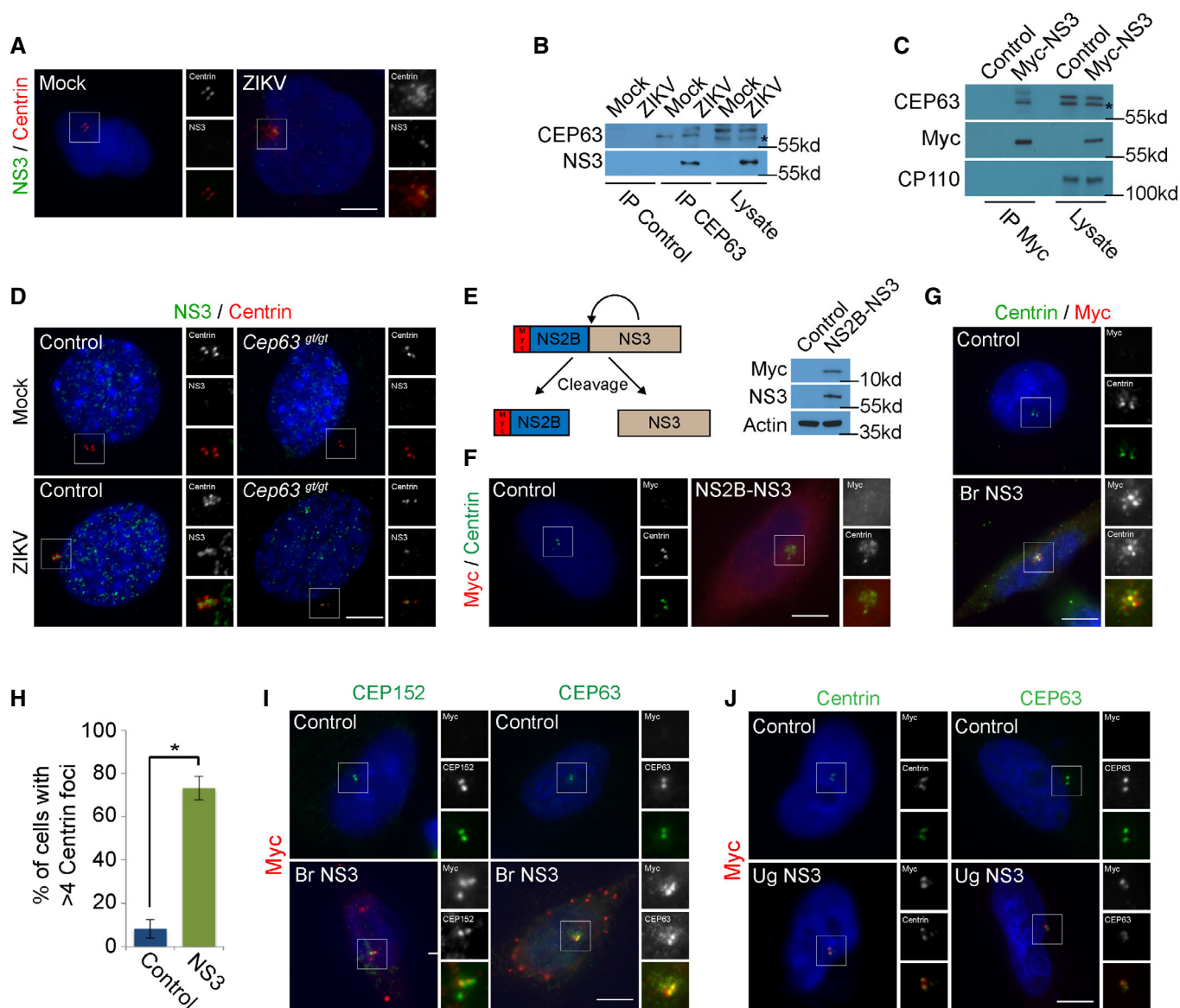


Figure 3. ZIKV NS3 binds the microcephaly-associated protein CEP63 and accumulates it at the centrosome.

- A Sixteen hours post infection mock or ZIKV-infected iNPC cells were co-stained for Centrin (red) and NS3 (green).
- B Mock or ZIKV-infected U87 cell lysates were immunoprecipitated for CEP63 or c-Myc, which served as a negative control for this and other immunoprecipitations (Control). Precipitated proteins were immunoblotted for CEP63 and NS3. Asterisk denotes specific band.
- C We expressed Myc-tagged Brazilian Zika NS3 in 293T/17 cells and immunoprecipitated c-Myc. Precipitated proteins were probed for the Myc tag of NS3 and endogenous CEP63. The centriole distal end component, CP110 served as a negative control. Asterisk denotes specific band for CEP63.
- D Mock and ZIKV-infected control and *Cep63^{gt/gt}* MEFs were co-stained for Centrin (red) and ZIKV NS3 (green).
- E Schematic representation of Myc-NS2B-NS3 being proteolytically cleaved by itself to generate Myc-NS2B and NS3 proteins. Immunoblot of HeLa cells transfected with Myc-NS2B-NS3 probed with antibodies to Myc and NS3. Actin served as a loading control.
- F Mock or Myc-NS2B-NS3 expressing HeLa cells co-stained for c-Myc (red) and Centrin (green).
- G HeLa cells transfected with Control or Myc-tagged Brazilian ZIKV NS3 (Br NS3) co-stained for Myc (red) and Centrin (green).
- H Quantification of the percentage of control and NS3 expressing HeLa cells with greater than four Centrin foci. Bars represent the mean \pm SD normalized to the control. For all quantifications, at least 100 cells were counted per experiment (biological replicates = 3). $P < 0.005$ (paired Student's t-test) for the comparison of NS3 to mock transfected cells was denoted with asterisk.
- I Control or Myc-tagged Brazilian ZIKV NS3 (Br NS3) transfected HeLa cells were co-stained for Myc (red) and MCPH protein CEP152 or CEP63.
- J Control or Myc-tagged Ugandan NS3 (Ug NS3) expressing HeLa cells were co-stained for Myc (red) and Centrin (green) or CEP63 (green).

Data information: Scale bars indicate 5 μ m for all images.

Source data are available online for this figure.

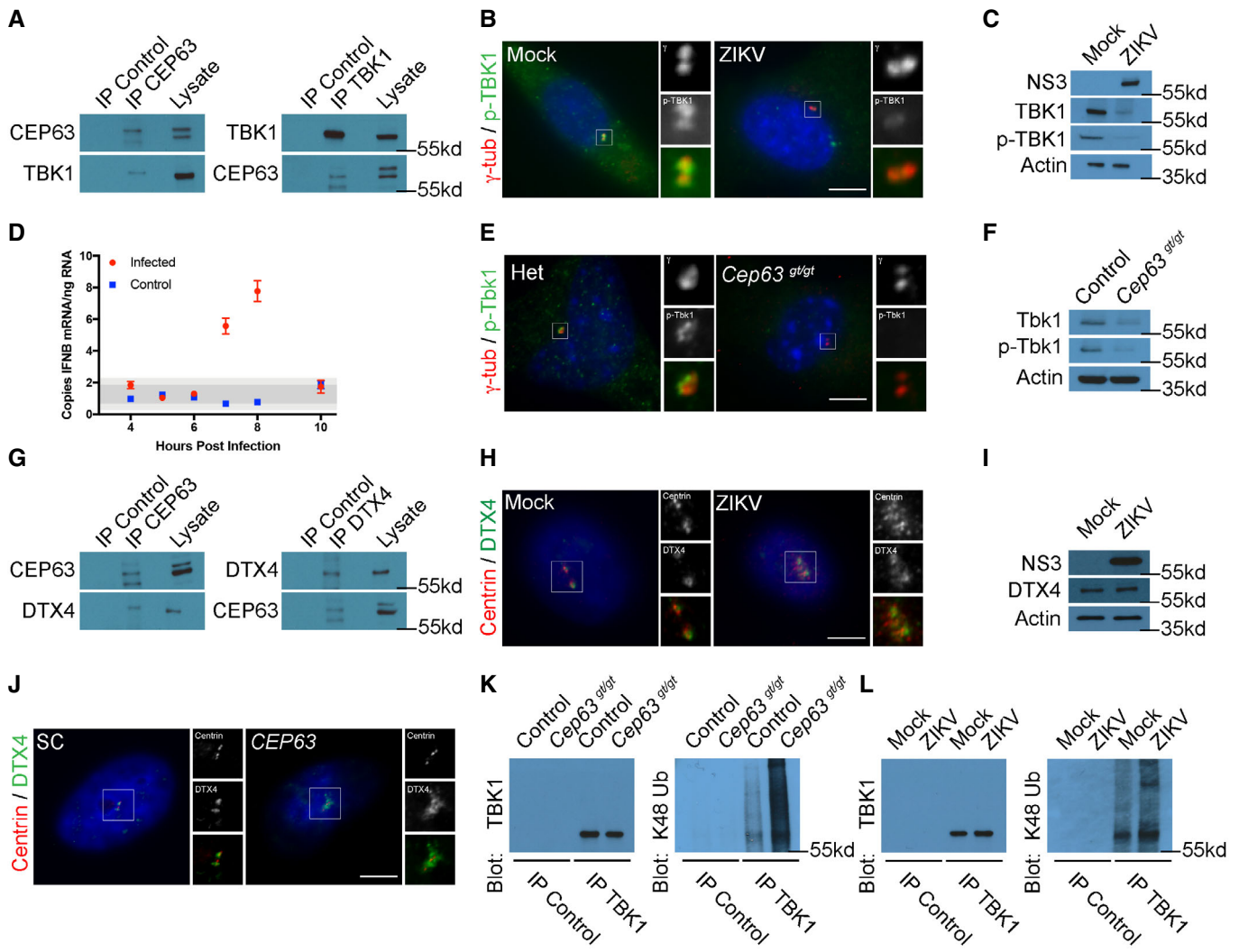


Figure 4. ZIKV degrades TBK1 to dampen the innate immune response.

- A HeLa cell lysates were immunoprecipitated with antibodies to CEP63 and TBK1. Precipitated proteins were immunoblotted for CEP63 and TBK1.
- B Mock and ZIKV-infected U87 cells were co-stained for γ -tubulin (red) and p-TBK1 (green).
- C Lysate from mock or ZIKV-infected U87 cells at 16 hpi were immunoblotted with antibodies to NS3, TBK1, and p-TBK1. Actin served as a loading control.
- D RT-ddPCR of IFN β transcript at the indicated time points in mock and ZIKV-infected H4 cells. Bars represent the mean \pm SD normalized to the control. Asterisk denotes $P < 0.005$ (Student's t -test). Three biological replicates are represented.
- E Control and *Cep63^{gt/gt}* MEFs were co-stained with antibodies to γ -tubulin (red) and p-Tbk1 (green).
- F Immunoblot analysis of control and *Cep63^{gt/gt}* MEFs probed with antibodies to Tbk1 and p-Tbk1. Actin served as a loading control.
- G HeLa cell lysate was immunoprecipitated with antibodies to CEP63, DTX4, or c-Myc (negative control). Precipitated proteins were blotted with antibodies to CEP63 and DTX4.
- H Mock and ZIKV-infected U87 cells co-stained for Centrin (red) and DTX4 (green).
- I Total cell lysate from mock and ZIKV-transfected U87 cells 16 hpi were analyzed by western blot using antibodies to ZIKV NS3 and DTX4. Actin served as a loading control.
- J SC and *CEP63* siRNA-treated HeLa cells were co-stained for Centrin (red) and DTX4 (green).
- K TBK1 or c-Myc (negative control) were immunoprecipitated from Control or *Cep63* mutant MEFs. Precipitating proteins were probed with antibodies to TBK1 and K48-linked ubiquitin.
- L Sixteen hours post infection Mock and ZIKV-infected U87 cell lysate was immunoprecipitated for TBK1 or c-Myc. The immunoprecipitations were probed using antibodies to TBK1 and K-48-linked ubiquitin.

Data information: Scale bars indicate 5 μ m for all images.

Source data are available online for this figure.

localization depends upon CEP63. Indeed, p-TBK1 and TBK1 were absent from centrosomes in *Cep63^{gt/gt}* MEFs (Figs 4E and EV4D–F), indicating that CEP63 is required for the centrosomal localization of

p-TBK1. Similarly, TBK1 and p-TBK1 levels were decreased in *Cep63^{gt/gt}* MEFs (Fig 4F). A similar reduction in TBK1 and p-TBK1 was observed in CEP63-depleted H4 and U87 cells (Fig EV4G and

H). These data are consistent with ZIKV interfering with CEP63 function to disrupt TBK1 stability.

How might ZIKV reorganize the centrosome in a CEP63-dependent manner to affect TBK1 stability? Once activated the innate immune response is attenuated by K48 ubiquitin-mediated degradation of TBK1 by the ubiquitin ligase DTX4 (Cui *et al.*, 2012). As TBK1 localizes to the centrosome, we examined whether DTX4 is present at centrosomes. Interestingly, DTX4 partially co-localized with γ -tubulin (Fig EV4I). The specificity of the antibody was confirmed by siRNA (Fig EV4I and J). In agreement with previously published data, depletion of DTX4 led to the stabilization of TBK1 (Cui *et al.*, 2012; Fig EV4J).

As TBK1 stability is disrupted in the absence of CEP63, we hypothesized that DTX4 interacts with and is localized to the

centrosome by CEP63. Reciprocal immunoprecipitation of CEP63 and DTX4 confirmed that these two proteins interact (Fig 4G). DTX4 accumulated in the vicinity of the centrosome in CEP63-depleted and ZIKV-infected cells (Figs 4H and J, and EV4K and M), suggesting that DTX4 interacts with, and its centrosomal localization is restricted by, CEP63. DTX4 accumulation was similarly observed in U87 and H4 cells depleted of CEP63 (Fig EV4L). Protein levels of DTX4 were unaltered in CEP63-depleted or ZIKV-infected cells (Figs 4I and EV4N). Thus, we hypothesized that inhibition of CEP63 function increases centrosomal DTX4 which, in turn, targets TBK1 for K48 ubiquitin-mediated degradation.

To test this hypothesis, we immunoprecipitated TBK1 from cells lacking Cep63 or infected with ZIKV and immunoblotted for K48-linked ubiquitin chains (Figs 4K and L, and EV4O and P). There

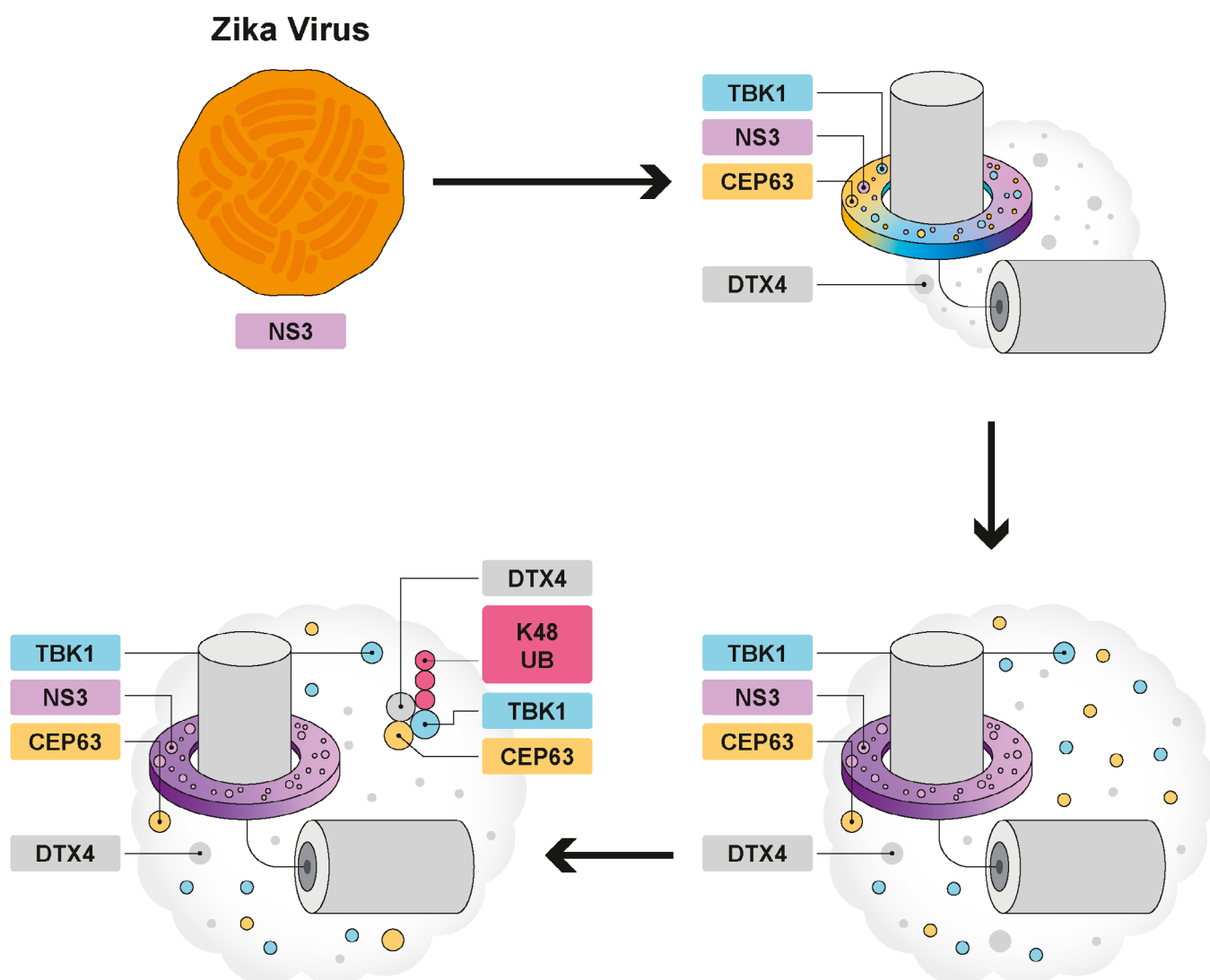


Figure 5. ZIKV NS3 alters centrosome organization to degrade TBK1.

The Brazilian ZIKV expressed NS3 protein localizes to the proximal end of the mother centriole where it interacts with the MCPH-associated protein, CEP63 and its interactors TBK1 and DTX4, regulators of the innate immune response. Centrosomal NS3 displaces the CEP63-TBK1-DTX4 away from the proximal centriole which forms an amorphous cloud in the proximity to the centrosome. Acentrosomal DTX4 K48-chain ubiquitylates TBK1 and targets it for proteasome-mediated degradation. Consequently, TBK1 is unable to activate the innate immune response pathway leading to the suppression of IFN β expression.

was a marked increase in K48-ubiquitylated TBK1 in *Cep63* mutant and ZIKV-infected cells suggesting that increased centrosomal DTX4 impacts the K48-ubiquitylation and degradation of TBK1. To determine whether the K48-ubiquitylation of TBK1 is centrosome-dependent, we immunoprecipitated TBK1 from SAS6 knockout cells that lack centrosomes (Wang *et al*, 2015). Contrary to ZIKV-infected and *Cep63^{gt/gt}* cells, there was a decrease in TBK1 K48-ubiquitylation in SAS6 knockout cells suggesting that TBK1 ubiquitylation depends upon the presence of centrosomes (Fig EV4Q). These findings suggest that ZIKV disrupts centrosomal CEP63 to alter the ubiquitylation and stability of TBK1 to dampen the innate immune response.

We have found that ZIKV-produced NS3 binds CEP63 to alter centrosome organization, but not centrosome amplification (Onorati *et al*, 2016), increases centrosomal DTX4, decreases TBK1 levels, and disrupts the innate immune response (Fig 5). As CEP63 mutations cause microcephaly in humans (Sir *et al*, 2011), disrupted CEP63 function may underlie the pathogenesis of ZIKV-associated microcephaly. Moreover, the centrosomal CEP63 interactor DTX4, regulator of neurogenic NOTCH signaling (Chastagner *et al*, 2017), is altered upon either loss of CEP63 or ZIKV infection. Based on these results, we propose that ZIKV NS3 disrupts CEP63 function to both dampen the innate immune response and potentially disrupt developmental signaling during brain development.

Previous studies have reported conflicting effects on centrosome biogenesis in ZIKV-infected cells (Onorati *et al*, 2016; Souza *et al*, 2016; Gabriel *et al*, 2017; Wolf *et al*, 2017; Kesari *et al*, 2020). Our results using human neural progenitor cells from fetal tissue, induced pluripotent stem cells, and established neural cell lines indicate that acute ZIKV infection disrupts centrosome organization but does not lead to centrosome amplification. As studies by others on centrosome biogenesis examined later time points following ZIKV infection, centrosomal overabundance in ZIKV-infected cells may be secondary to multiple rounds of abnormal cell division.

We found that ZIKV-produced NS3 localizes to the centrosome to induce the formation of supernumerary Centrin foci by interacting with and localizing increased amounts of CEP63 to the centrosome. The failure of ZIKV infection in *Cep63* mutant MEFs to induce supernumerary Centrin supports our assertion that ZIKV disrupts centrosome organization in a CEP63-dependent manner.

We and others have shown that CEP63 promotes centriole duplication (Loffler *et al*, 2011; Sir *et al*, 2011; Brown *et al*, 2013; Kodani *et al*, 2015). However, its function in other cellular processes has not been explored. Here, we have provided evidence that CEP63 controls TBK1 stability, a central component of innate immune signaling. Given that CEP63 interacts with and limits the localization of the centrosomal ubiquitin ligase DTX4, to the centrosome, a direct role for CEP63 in promoting cellular signaling at the centrosome is implicit.

We found that DTX4 localizes to the centrosome and promotes the K48-ubiquitylation of TBK1. DTX4 accumulates at the centrosome in ZIKV-infected cells in a CEP63-dependent manner. As TBK1 is ubiquitylated by DTX4 to promote its degradation, we propose that ZIKV-mediated recruitment of DTX4 to the centrosome may limit TBK1 activity and stability, and thus the innate immune response, to ZIKV infection. It will be interesting to determine whether other viruses with NS3 homologs such as SARS-CoV-2 M^{Pro} and NSP13 which interact with centrosome proteins (preprint:

Gordon *et al*, 2020) can similarly suppress innate immunity by altering centrosome organization.

In summary, we have found that ZIKV NS3 localizes to the centrosome, disrupts CEP63 function and its binding partner DTX4 to ubiquitylate and degrade TBK1, a key regulator of the innate immune response. These findings provide mechanistic insight into how ZIKV specifically targets the centrosome with implications for how it may both evade viral detection.

Materials and Methods

Cell culture and transfection

HeLa and 293T/17 cells (UCSF Tissue Culture Facility) were cultured in Advanced Dulbecco's Modified Eagle's medium (DMEM, Thermo Fisher Scientific) supplemented with 2% fetal bovine serum (FBS, Thermo Fisher Scientific) and Glutamax-I (Thermo Fisher Scientific). U87 and H4 cells were cultured in DMEM (Thermo Fisher Scientific) supplemented with 10% FBS and L-glutamine (Thermo Fisher Scientific). *Cep63^{gt/gt}* MEFs and control *Cep90^{+/-}* MEFs were cultured in Amniomax C-100 (Thermo Fisher Scientific). *p53^{+/-}* and *p53^{-/-} SAS6^{-/-}* hTERT-RPE1 cells (Wang *et al*, 2015) were grown in DMEM/F-12 media (Thermo Fisher Scientific) supplemented with 10% FBS and Glutamax-I (Thermo Fisher Scientific). 293T/17 and HeLa cells were transfected with plasmids using FugeneHD (Promega) or Lipofectamine3000 (Thermo Fisher Scientific), respectively, according to the manufacturer's instructions and analyzed 8 h later. NPCs were derived from pluripotent stem cells (NIH Human Embryonic Stem Cell Registry line WA09 (H9) at passages 30–35) according to a recently published protocol (Krencik *et al*, 2015) and maintained in neural media composed of DMEM/F12 with sodium pyruvate and Glutamax, N2, B27, heparin and antibiotics. Medium was either supplemented with growth factors epidermal growth factor (10 ng/ml) and fibroblast growth factor (10 ng/ml).

Fetal tissue collection, dissociation and culture

De-identified fetal brain tissue samples were collected with previous patient consent in strict observance of the legal and institutional ethical regulations from elective pregnancy termination specimens at San Francisco General Hospital. Protocols were approved by the Human Gamete, Embryo and Stem Cell Research Committee (an institutional review board) at the University of California, San Francisco. Blocks of cortical tissue spanning the ventricle to the cortical plate were dissected away from meninges and germinal zone using a stereomicroscope, and then minced using a razor blade. Cells were dissociated by incubation with Papain (Worthington Biochemical Corporation) at 37°C for 30–40 min, followed by the addition of DNase I and trituration. The cells were collected by centrifugation for 5 min at 300 g, the supernatant was removed, and the cells were resuspended in sterile DMEM containing N-2, B-27 supplement, penicillin, streptomycin and glutamine and sodium pyruvate (0.11 mg/ml; all Invitrogen). The suspension was passed through a 40 µm strainer (BD Falcon) to yield a uniform suspension of single cells. Cells were plated at a density of 1.5×10^6 cells/well on 18 mm coverslips (Neuvitro 18-GG-PDL) precoated with high

concentration growth factor-reduced Matrigel (BDBiosciences, 354263) and cultured at 37°C, 5% CO₂, 8% O₂.

Virus and infections

ZIKV strain PRVABC59 was propagated in Vero cells. Viral titers were determined by focus assay (Battagay *et al*, 1991). Briefly, serial dilutions of viral stock were added to Vero cells in 96-well plates. Twenty-four hours post infection, inoculum was removed and cells were fixed with 3.7% PFA for 15 min. Foci were visualized by immunofluorescent staining for flavivirus envelope. ZIKV infections of NPCs, U87, and H4 cell lines, at MOIs of 10, were carried out by incubating cells with inoculum for 1 h and then replacing the inoculum with fresh media. ZIKV was added to dissociated fetal brain cells at MOIs of 10 and incubated for 16 h unless stated otherwise. Mock and ZIKV-infected cells were fixed 12–16 h post infection in chilled methanol for 3 min at –20°C and processed for immunofluorescence.

Molecular biology

Wild-type human codon optimized ZIKV NS2B3 and NS3 open reading frame flanked by attB sites were synthesized by Gibson assembly (SGI). Gateway cloning into pDONR221 generated pENTR-NS3 ZIKV. Subsequent Gateway-mediated subcloning into pDEST-CMV-Myc (gift of Keith Yamamoto) generated pCMV-Myc-NS3 Brazilian and Ugandan ZIKV, encoding N-terminally Myc-tagged NS3 and pCMV-Myc-NS2B3 Brazilian ZIKV encoding an N-terminally Myc-tagged fusion of NS2B and NS3. The S135A mutant form of NS3 was generated using site-directed mutagenesis to create pCMV-Myc-NS3-S135A Brazilian ZIKV (QuikChange II, Agilent).

Biochemistry

Immunoprecipitations were performed as previously described (Kodani *et al*, 2013). In brief, mock or ZIKV-infected U87 cells or 293T/17 cells were collected in Dulbecco's phosphate-buffered saline (DPBS), lysed in lysis buffer (1% IGEPAL CA-630, 50 mM Tris-HCl pH 7.4, 266 mM NaCl, 2.27 mM KCl, 1.25 mM KH₂PO₄, 6.8 mM Na₂HPO₄·7H₂O) supplemented with protease and phosphatase inhibitors (EMD Millipore). Myc-tagged proteins were immunoprecipitated with 4AG Myc monoclonal agarose beads (EMD Millipore), washed three times in lysis buffer and boiled in 2× Laemmli reducing buffer (Bio-Rad). Samples were separated on 4–15% TGX precast gels (Bio-Rad), transferred onto Protran BA85 nitrocellulose membrane (GE Healthcare) and subsequently analyzed by immunoblot using ECL Lightening PLUS (Perkin-Elmers) or SuperSignal West Dura (Thermo Fisher Scientific).

Immunofluorescence microscopy

Cells were fixed in –20°C methanol for 3 min followed by permeabilization in blocking buffer (2.5% BSA, 0.1% Triton-X100, 0.03% NaN₃ in DPBS) for 30 min. Primary and secondary antibodies (Table 1) were diluted in blocking buffer and incubated with cells for at least 1 h. To detect cells in S-phase, cells were co-stained with antibodies to Centrin and Cyclin A to determine centriole number and S-phase/G2 cells, respectively. To detect TBK1 and Phospho-TBK1, U87 and MEFs were fixed in 4% paraformaldehyde for 30 min, blocked in

Table 1. Antibodies used in the study.

Target	Dilution	Species	Source
Flavivirus envelope	1:500	Mouse	Millipore MAB10216
Centrin	1:1,000	Mouse	Millipore 04-1624
Centrin 3	1:1,000	Rabbit	Proteintech 15811-1-AP
SOX2	1:250	Goat	Santa Cruz SC-17320
γ-tubulin	1:1,000 (WB/IF)	Rabbit	Sigma T5192
γ-tubulin	1:500	Mouse	Sigma T5326
Pericentrin	1:2,000	Rabbit	Abcam ab4448
CP110	1:2,000	Rabbit	Proteintech 12780-1-AP
CEP164	1:500	Goat	Santa Cruz sc-240226
PLK4	1:1,000	Rabbit	Dr. Andrew Holland
STIL	1:1,000	Rabbit	Dr. Andrew Holland
STIL	1:2,000 (WB)	Rabbit	Bethyl A302-441
SAS6	1:1,000	Rabbit	Dr. Alexander Dammermann
SAS6	1:2,000 (WB)	Mouse	Santa Cruz SC-81431
CEP90	1:1,000 (IF)	Rabbit	Proteintech 14413-1-AP
CDK5RAP2	1:2,000	Rabbit	Millipore 06-1387
CEP152	1:2,000	Rabbit	Bethyl A302-480
WDR62	1:500	Rabbit	Bethyl A301-559
WDR62	1:5,000 (WB)	Rabbit	Bethyl A301-560
CEP63	1:500 (WB/IF)	Rabbit	Millipore 06-1292
CEP63	1:1,000 (IF)	Rabbit	Proteintech 16268-1-AP
c-Myc-488	1:1,000	Mouse	Millipore 16-224
c-Myc	1:1,000	Mouse	Millipore 05-724
CyclinA	1:500	Rabbit	Santa Cruz SC-751
DTX4	1:500 (WB/IF)	Rabbit	Genetex GTX31606
Actin	1:2,000 (WB)	Rabbit	Proteintech 20536-1-AP
Calreticulin	1:200 (IF)	Rabbit	Abcam AB2907
P53	1:1,000 (WB)	Mouse	Santa Cruz SC-126
NS3	1:1,000	Rabbit	Thermo Fisher PA5-32199
K63 Ubiquitin	1:500 (WB)	Rabbit	Millipore 05-1308
K63 Ubiquitin	1:500 (WB)	Rabbit	Abcam
K48 Ubiquitin	1:500 (WB)	Rabbit	Millipore
K48 Ubiquitin	1:500 (WB)	Rabbit	Abcam
TBK1	1:1,000 (WB)	Rabbit	Cell Signal 3504S
TBK1	1:100 (IP) 1:50 (IF)	Rabbit	Cell Signal 3013S
p-TBK1 (Ser172)	1:1,000 (WB) 1:50 (IF)	Rabbit	Cell Signal 5483S

5% FBS and 0.5% TritonX100 diluted in DPBS. Permeabilized cells were stained overnight at room temperature using the TBK1 or p-TBK1 antibody at a dilution of 1:50 in 5% FBS and 0.1% TritonX100

Table 2. Primers used in the study.

Name	Sequence
Cep63-WT L	5'-gtaggaccaggccttagcgtag-3'
Cep63-WT R	5'-tgaaccttcagcatatcac-3'
Cep63 gt L	5'-gtaggaccaggccttagcgtag-3'
Cep63 gt R	5'-caaggcgattaagttgggtaacg-3'
Forward IFN β	5'-gatgacggagaagatgcagaag-3'
Reverse IFN β	5'-accagtgctggagaaattg-3'
Probe IFN β	5'-/5hex/acactgcct/zen/ttgccatccaagaga/3iabkfq/-3'

diluted in DPBS. Samples were mounted in Gelvatol or Prolong Glass and imaged with an Axio Observer D1 or LSM900 (Zeiss). Images were processed using Adobe Photoshop and analyzed using Fiji.

RT-ddPCR

RNA was isolated from infected cells at various time points post infection using Trizol (Invitrogen) and Direct-zol RNA Miniprep kits (Zymo Research). Droplets containing RNA, One-Step RT-ddPCR Advanced Kit for Probes (Bio-Rad Laboratories), and probes were prepared on a QX200 Droplet Generator (Bio-Rad Laboratories), using Droplet Generation Oil for Probes (Bio-Rad Laboratories). RT-PCR was run in droplets on a C1000 Touch (Bio-Rad Laboratories) following the manufactures' direction for One-Step RT-ddPCR Advanced Kit for Probes. Droplets were read on a QX100 Droplet Reader (Bio-Rad Laboratories). Primers: Forward IFN β 5'-GAT GACGGAGAAGATGCAGAAG-3', Reverse IFN β 5'-ACCCAGTGCTG GAGAAATTG-3'. The probe was designed using the Primer Quest Tool from IDT and used 5'6'FAM/ZEN/3'IBFQ (IDT): 5'-/5HEX/ACACTGCCT/ZEN/TTGCCATCCAAGAGA/3IABKfq/-3' (Table 2).

Data availability

No data were deposited in a public database.

Expanded View for this article is available online.

Acknowledgements

We thank Drs. Alexander Dammermann, Travis Stracker, Bryan Meng-Fu Tsou, and Andrew Holland for antibodies and cell lines. We also thank Drs. Emanuela Gussoni, Joseph Gleeson, and Nevan Krogan for insightful discussions. A.T.K. was supported by National Institute of Health R21NS104633-01A1, the William Randolph Hearst Fund, and the Charles Hood Foundation. J.F.R. and this work was supported by National Institute of Health R01R01DE029454 and R01AR054396. H.R. was supported by National Institute of Health NINDS F31NS108615. J.D. is supported by the Chan Zuckerberg Initiative. A.K. was supported by National Institute of Health U01MH114825 and 3R35NS097305, the California Institute of Regenerative Medicine GC1R-06673-C, and A.R. would like to thank Marc and Lynne Benioff for their financial support. The content is solely the responsibility of the authors and does not represent the official views of the National Institute of Health.

Author contributions

Andrew Kodani: Conceptualization; resources; data curation; formal analysis; supervision; funding acquisition; validation; investigation; visualization;

methodology; writing – original draft; project administration; writing – review and editing. **Kristeene A Knopp:** Data curation; formal analysis; investigation; methodology. **Elizabeth Di Lullo:** Data curation. **Hanna Retallack:** Data curation. **Arnold R Kriegstein:** Methodology. **Joseph L DeRisi:** Data curation; investigation; methodology. **Jeremy F Reiter:** Data curation; supervision; funding acquisition; methodology; writing – review and editing.

In addition to the [CRediT](#) author contributions listed above, the contributions in detail are:

The project was conceived by AKo and JFR, and the experiments were carried out by AKo and KAK who had comparable contributions to this study regarding cell biology and virology, respectively. EDL and HR contributed to the collection and processing of embryonic samples and virology, respectively. Data analysis was performed by AKo, KAK, JFR, and JLDR. The manuscript was written by AKo with help from the other authors. All aspects of the study were supervised by AKo and JFR. All authors approved the manuscript.

Disclosure and competing interests statement

The authors declare that they have no conflict of interest.

References

- Battegay M, Cooper S, Althage A, Banziger J, Hengartner H, Zinkernagel RM (1991) Quantification of lymphocytic choriomeningitis virus with an immunological focus assay in 24- or 96-well plates. *J Virol Methods* 33: 191–198
- Bazzi H, Anderson KV (2014) Acentriolar mitosis activates a p53-dependent apoptosis pathway in the mouse embryo. *Proc Natl Acad Sci USA* 111: E1491–E1500
- Bera AK, Kuhn RJ, Smith JL (2007) Functional characterization of cis and trans activity of the flavivirus NS2B-NS3 protease. *J Biol Chem* 282: 12883–12892
- Bertipaglia C, Goncalves JC, Vallee RB (2018) Nuclear migration in mammalian brain development. *Semin Cell Dev Biol* 82: 57–66
- Brown NJ, Marjanovic M, Luders J, Stracker TH, Costanzo V (2013) Cep63 and cep152 cooperate to ensure centriole duplication. *PLoS ONE* 8: e69986
- Calvet G, Aguiar RS, Melo ASO, Sampaio SA, de Filippis I, Fabri A, Araujo ESM, de Sequeira PC, de Mendonca MCL, de Oliveira L et al (2016) Detection and sequencing of Zika virus from amniotic fluid of fetuses with microcephaly in Brazil: a case study. *Lancet Infect Dis* 16: 653–660
- Chastagner P, Rubinstein E, Brou C (2017) Ligand-activated Notch undergoes DTX4-mediated ubiquitylation and bilateral endocytosis before ADAM10 processing. *Sci Signal* 10: eaag2989
- Coyaud E, Ranadheera C, Cheng D, Goncalves J, Dyakov BJA, Laurent EMN, St-Germain J, Pelletier L, Gingras AC, Brumell JH et al (2018) Global Interactomics uncovers extensive organellar targeting by Zika virus. *Mol Cell Proteomics* 17: 2242–2255
- Cui J, Li Y, Zhu L, Liu D, Songyang Z, Wang HY, Wang RF (2012) NLRP4 negatively regulates type I interferon signaling by targeting the kinase TBK1 for degradation via the ubiquitin ligase DTX4. *Nat Immunol* 13: 387–395
- Farlik M, Rapp B, Marie I, Levy DE, Jamieson AM, Decker T (2012) Contribution of a TANK-binding kinase 1-interferon (IFN) regulatory factor 7 pathway to IFN-gamma-induced gene expression. *Mol Cell Biol* 32: 1032–1043

- Ferraris P, Cochet M, Hamel R, Gladwyn-Ng I, Alfano C, Diop F, Garcia D, Talignani L, Montero-Menei CN, Nougairede A et al (2019) Zika virus differentially infects human neural progenitor cells according to their state of differentiation and dysregulates neurogenesis through the Notch pathway. *Emerg Microbes Infect* 8: 1003–1016
- Fitzgerald KA, McWhirter SM, Faia KL, Rowe DC, Latz E, Golenbock DT, Coyle AJ, Liao SM, Maniatis T (2003) IKKepsilon and TBK1 are essential components of the IRF3 signaling pathway. *Nat Immunol* 4: 491–496
- Gabriel E, Ramani A, Karow U, Gottardo M, Natarajan K, Gooi LM, Goranci-Buzhala G, Krut O, Peters F, Nikolic M et al (2017) Recent Zika virus isolates induce premature differentiation of neural progenitors in human brain organoids. *Cell Stem Cell* 20: e395
- Gonczy P, Hatzopoulos GN (2019) Centriole assembly at a glance. *J Cell Sci* 132: jcs228833
- Gordon DE, Jang GM, Bouhaddou M, Xu J, Obernier K, O'Meara MJ, Guo JZ, Swaney DL, Tummino TA, Huttenhain R et al (2020) A SARS-CoV-2-human protein-protein interaction map reveals drug targets and potential drug-repurposing. *bioRxiv* <https://doi.org/10.1101/2020.03.22.002386> [PREPRINT]
- Graser S, Stierhof YD, Lavoie SB, Gassner OS, Lamla S, Le Clech M, Nigg EA (2007) Cep164, a novel centriole appendage protein required for primary cilium formation. *J Cell Biol* 179: 321–330
- Gupta GD, Coyaud E, Goncalves J, Mojarad BA, Liu Y, Wu Q, Gheiratmand L, Comartin D, Tkach JM, Cheung SW et al (2015) A dynamic protein interaction landscape of the human centrosome-cilium Interface. *Cell* 163: 1484–1499
- Helgason E, Phung QT, Dueber EC (2013) Recent insights into the complexity of Tank-binding kinase 1 signaling networks: the emerging role of cellular localization in the activation and substrate specificity of TBK1. *FEBS Lett* 587: 1230–1237
- Hou W, Cruz-Cosme R, Armstrong N, Obwolo LA, Wen F, Hu W, Luo MH, Tang Q (2017) Molecular cloning and characterization of the genes encoding the proteins of Zika virus. *Gene* 628: 117–128
- Hu WF, Pomp O, Ben-Omran T, Kodani A, Henke K, Mochida GH, Yu TW, Woodworth MB, Bonnard C, Raj GS et al (2014) Katanin p80 regulates human cortical development by limiting centriole and cilia number. *Neuron* 84: 1240–1257
- Jayaraman D, Bae BI, Walsh CA (2018) The genetics of primary microcephaly. *Annu Rev Genomics Hum Genet* 19: 177–200
- Jayaraman D, Kodani A, Gonzalez DM, Mancias JD, Mochida GH, Vagnoni C, Johnson J, Krogan N, Harper JW, Reiter JF et al (2016) Microcephaly proteins Wdr62 and Aspm define a mother centriole complex regulating centriole biogenesis, apical complex, and cell fate. *Neuron* 92: 813–828
- Kesari AS, Heintz VJ, Poudyal S, Miller AS, Kuhn RJ, LaCount DJ (2020) Zika virus NS5 localizes at centrosomes during cell division. *Virology* 541: 52–62
- Khadka S, Vangeloff AD, Zhang C, Siddavatam P, Heaton NS, Wang L, Sengupta R, Sahasrabudhe S, Randall G, Gribskov M et al (2011) A physical interaction network of dengue virus and human proteins. *Mol Cell Proteomics* 10: M111.012187
- Khan MA, Rupp VM, Orpinell M, Hussain MS, Altmuller J, Steinmetz MO, Enzinger C, Thiele H, Hohne W, Nurnberg G et al (2014) A missense mutation in the PISA domain of HsSAS-6 causes autosomal recessive primary microcephaly in a large consanguineous Pakistani family. *Hum Mol Genet* 23: 5940–5949
- Kim TS, Zhang L, Il Ahn J, Meng L, Chen Y, Lee E, Bang JK, Lim JM, Ghirlando R, Fan L et al (2019) Molecular architecture of a cylindrical self-assembly at human centrosomes. *Nat Commun* 10: 1151
- Kodani A, Salome Sierrol-Piquet M, Seol A, Garcia-Verdugo JM, Reiter JF (2013) Kif3a interacts with dynein subunit p150 glued to organize centriole subdistal appendages. *EMBO J* 32: 597–607
- Kodani A, Yu TW, Johnson JR, Jayaraman D, Johnson TL, Al-Gazali L, Sztrihai L, Partlow JN, Kim H, Krup AL et al (2015) Centriolar satellites assemble centrosomal microcephaly proteins to recruit CDK2 and promote centriole duplication. *eLife* 4: e07519
- Krencik R, Hokanson KC, Narayan AR, Dvornik J, Rooney GE, Rauen KA, Weiss LA, Rowitch DH, Ullian EM (2015) Dysregulation of astrocyte extracellular signaling in Costello syndrome. *Sci Transl Med* 7: 286ra266
- Kumar A, Girmaji SC, Duvvari MR, Blanton SH (2009) Mutations in STIL, encoding a pericentriolar and centrosomal protein, cause primary microcephaly. *Am J Hum Genet* 84: 286–290
- Lawo S, Hasegan M, Gupta GD, Pelletier L (2012) Subdiffraction imaging of centrosomes reveals higher-order organizational features of pericentriolar material. *Nat Cell Biol* 14: 1148–1158
- Le Breton M, Meyniel-Schicklin L, Deloire A, Coutard B, Canard B, de Lamballerie X, Andre P, Rabourdin-Combe C, Lotteau V, Davoust N (2011) Flavivirus NS3 and NS5 proteins interaction network: a high-throughput yeast two-hybrid screen. *BMC Microbiol* 11: 234
- Li S, Wang L, Berman M, Kong YY, Dorf ME (2011) Mapping a dynamic innate immunity protein interaction network regulating type I interferon production. *Immunity* 35: 426–440
- Liu D, Sheng C, Gao S, Yao C, Li J, Jiang W, Chen H, Wu J, Pan C, Chen S et al (2015) SOCS3 drives proteasomal degradation of TBK1 and negatively regulates antiviral innate immunity. *Mol Cell Biol* 35: 2400–2413
- Loffler H, Fechter A, Matuszewska M, Saffrich R, Mistrik M, Marhold J, Hornung C, Westermann F, Bartek J, Kramer A (2011) Cep63 recruits Cdk1 to the centrosome: implications for regulation of mitotic entry, centrosome amplification, and genome maintenance. *Cancer Res* 71: 2129–2139
- Martin CA, Ahmad I, Klingseisen A, Hussain MS, Bicknell LS, Leitch A, Nurnberg G, Toliat MR, Murray JE, Hunt D et al (2014) Mutations in PLK4, encoding a master regulator of centriole biogenesis, cause microcephaly, growth failure and retinopathy. *Nat Genet* 46: 1283–1292
- Mlakar J, Korva M, Tul N, Popovic M, Poljsak-Prijatelj M, Mraz J, Kolenc M, Resman Rus K, Vesnaver Vipotnik T, Fabjan Vodusek V et al (2016) Zika virus associated with microcephaly. *N Engl J Med* 374: 951–958
- Nano M, Basto R (2017) Consequences of centrosome dysfunction during brain development. *Adv Exp Med Biol* 1: 19–45
- Onorati M, Li Z, Liu F, Sousa AMM, Nakagawa N, Li M, Dell'Anno MT, Gulden FO, Pochareddy S, Tebbenkamp ATN et al (2016) Zika virus disrupts Phospho-TBK1 localization and mitosis in human neuroepithelial stem cells and radial glia. *Cell Rep* 16: 2576–2592
- Paoletti A, Moudjou M, Paintrand M, Salisbury JL, Bornens M (1996) Most of centrin in animal cells is not centrosome-associated and centrosomal centrin is confined to the distal lumen of centrioles. *J Cell Sci* 109: 3089–3102
- Perry AK, Chow EK, Goodnough JB, Yeh WC, Cheng G (2004) Differential requirement for TANK-binding kinase-1 in type I interferon responses to toll-like receptor activation and viral infection. *J Exp Med* 199: 1651–1658
- Pillai S, Nguyen J, Johnson J, Haura E, Coppola D, Chellappan S (2015) Tank binding kinase 1 is a centrosome-associated kinase necessary for microtubule dynamics and mitosis. *Nat Commun* 6: 10072
- Saade M, Blanco-Ameijeiras J, Gonzalez-Gobartt E, Marti E (2018) A centrosomal view of CNS growth. *Development* 145: dev170613
- Sharma S, tenOever BR, Grandvaux N, Zhou GP, Lin R, Hiscott J (2003) Triggering the interferon antiviral response through an IKK-related pathway. *Science* 300: 1148–1151
- Sir JH, Barr AR, Nicholas AK, Carvalho OP, Khurshid M, Sossick A, Reichelt S, D'Santos C, Woods CG, Gergely F (2011) A primary microcephaly protein complex forms a ring around parental centrioles. *Nat Genet* 43: 1147–1153

- Sonnen KF, Gabryjonczyk AM, Anselm E, Stierhof YD, Nigg EA (2013) Human Cep192 and Cep152 cooperate in Plk4 recruitment and centriole duplication. *J Cell Sci* 126: 3223–3233
- Souza BS, Sampaio GL, Pereira CS, Campos GS, Sardi SI, Freitas LA, Figueira CP, Paredes BD, Nonaka CK, Azevedo CM *et al* (2016) Zika virus infection induces mitosis abnormalities and apoptotic cell death of human neural progenitor cells. *Sci Rep* 6: 39775
- Spektor A, Tsang WY, Khoo D, Dynlacht BD (2007) Cep97 and CP110 suppress a cilia assembly program. *Cell* 130: 678–690
- Stearns T, Evans L, Kirschner M (1991) Gamma-tubulin is a highly conserved component of the centrosome. *Cell* 65: 825–836
- Varadarajan R, Rusan NM (2018) Bridging centrioles and PCM in proper space and time. *Essays Biochem* 62: 793–801
- Wang L, Li S, Dorf ME (2012) NEMO binds ubiquitinated TANK-binding kinase 1 (TBK1) to regulate innate immune responses to RNA viruses. *PLoS ONE* 7: e43756
- Wang WJ, Acehan D, Kao CH, Jane WN, Uryu K, Tsou MF (2015) De novo centriole formation in human cells is error-prone and does not require SAS-6 self-assembly. *eLife* 4: e10586
- Wolf B, Diop F, Ferraris P, Wichit S, Busso C, Misse D, Gonczy P (2017) Zika virus causes supernumerary foci with centriolar proteins and impaired spindle positioning. *Open Biol* 7: 160231
- Xing H, Xu S, Jia F, Yang Y, Xu C, Qin C, Shi L (2020) Zika NS2B is a crucial factor recruiting NS3 to the ER and activating its protease activity. *Virus Res* 275: 197793
- Zhang R, Miner JJ, Gorman MJ, Rausch K, Ramage H, White JP, Zuiani A, Zhang P, Fernandez E, Zhang Q *et al* (2016) A CRISPR screen defines a signal peptide processing pathway required by flaviviruses. *Nature* 535: 164–168
- Zhu Z, Chan JF, Tee KM, Choi GK, Lau SK, Woo PC, Tse H, Yuen KY (2016) Comparative genomic analysis of pre-epidemic and epidemic Zika virus strains for virological factors potentially associated with the rapidly expanding epidemic. *Emerg Microbes Infect* 5: e22